Anthracene-Functionalized Polystyrene Random Copolymers: Effects of Side-Chain Modification on Polymer Structure and Behavior

Roy Shenhar, Amitav Sanyal, Oktay Uzun, and Vincent M. Rotello*

Department of Chemistry, University of Massachusetts, Amherst, Massachusetts 01003

Received October 2, 2003; Revised Manuscript Received October 30, 2003

ABSTRACT: Copolymers consisting of styrene and 4-chloromethylstyrene (CMS) were functionalized via reaction with 9-anthracenecarboxylic acid, providing the corresponding esters. Increasing degrees of functionalization were found to increase the glass transition temperature, influence chain packing density, and induce microphase separation in block copolymer structures. The approach demonstrated in this study facilitates the investigation of the relationship between structure of side-chain groups and polymer properties, providing a general approach for the study of the effect of chemical functionality on material properties of polymers.

Introduction

Introducing chemical functionality to polymers provides access to a wide variety of material properties that stem from the functional groups used. Examples are numerous, including attachment of charged functionalities to polymers to assemble polymer films by the layer-by-layer deposition technique,[1] which finds applications such as superior light-emitting diodes (LED)[2] and in the creation of hollow capsules.[3] Other examples include the use of functionalities capable of molecular recognition to create novel composite materials[4] and molecularly imprinted matrices for sensor applications,[5] side-chain functionalization for the creation of reactive membranes,[6] and reactive side-chain groups functionalized on block copolymers that can be used for surface modification.[7]

The phenomenon of microphase separation of block copolymers, on the other hand, affords the possibility to create well-defined periodic microdomains of controlled morphologies (e.g., cylinders, spheres, lamellae) on the 10−100 nm scale, a key size scale for emerging technologies.[8] The size and morphology of the domains are dictated by the relative block lengths as well as by the strength of interaction between the polymer segments. In this sense, polymer functionalization can be used to adjust both segment−segment interactions[9] and block volume fractions and thus offers another handle to control phase architecture.[10]

The study presented in this paper is aimed at probing the effect of side-chain functionality on general polymer behavior as well as on microphase separation in block copolymers.[9,11] There are two ways to introduce functionality to a polymer backbone: polymerization of a prefunctionalized monomer and attachment of functionality to a preformed polymer scaffold via postpolymerization reactions. We chose the second approach, which affords the following three advantages: (a) applicability to a wide variety of functions (while in the first method the modified monomer may unfavorably intervene in the polymerization reaction[12]), (b) ability to create random copolymers with close-to-statistical comonomer distribution by copolymerization of similar comonomers (of which one is a functionalizable monomer), thus avoiding "blockiness" that may arise from associative processes of like monomers when very different monomers are copolymerized, and (c) ability to use the exact same polymer scaffold for the attachment of different functions, which allows isolation and comparison of the functionality contribution to the polymer behavior.

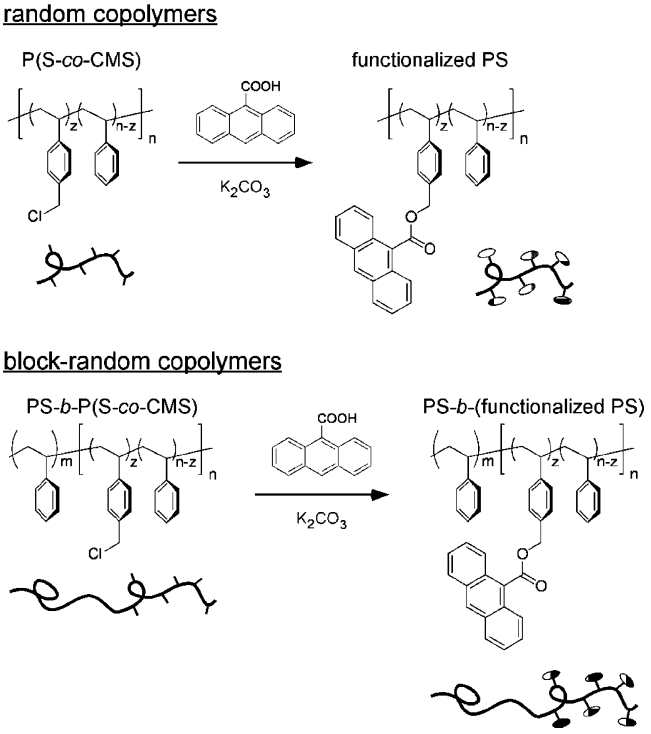

Figure 1. Functionalization approach used in the synthesis of Anth-functionalized monoblock and diblock copolymers.

The general polymer scaffolds used in this study consist of monomers of styrene (S) and 4-chloromethylstyrene (CMS). The CMS units provide the handles for functionality attachment through nucleophilic substitution (Figure 1), which was employed in numerous studies.[6,13] Copolymerization of CMS in low molar ratios with styrene allows envisioning the functionalized polymer as composed of a polystyrene (PS) backbone and an attached functionality and also affords easier processing during and after functionalization.[14]

* To whom correspondence should be addressed: Tel (413) 545-2058; Fax (413) 545-4490; e-mail rotello@chem.umass.edu.

10.1021/ma035488d CCC: $27.50
Published on Web 12/10/2003

Table 1. Molecular Attributes of Parent P(S-*co*-CMS) and PS-*b*-P(S-*co*-CMS) Polymer Scaffolds

notation	series	M_n (kg/mol)[a]			PDI[a]	DP[a,c,d]	functionality content (mol %)[a,d,e]
		PS[b]	P(S-*co*-CMS)	total			
PS/CMS(19,20%)			18.5	18.5	1.28	163	20
PS/CMS(25,50%)			24.8	24.8	1.46	194	50
PS/CMS(27:13,17%)	A	27.3	12.8	40.1	1.26	377	17
PS/CMS(27:13,25%)	A, B	27.1	12.7	39.8	1.16	370	25
PS/CMS(28:13,40%)	A	27.8	13.2	41.0	1.25	374	40
PS/CMS(27:20,25%)	B	27.1	20.1	47.2	1.23	434	25
PS/CMS(27:23,20%)	B	27.1	23.1	50.2	1.23	464	20
PS/CMS(27:26,22%)	B	27.1	26.2	53.3	1.25	489	22

[a] According to SEC with PS standards. [b] PDI of all PS blocks were ca. 1.1. [c] Average total degree of polymerization. [d] Calculated from ^{1}H NMR integration. [e] Molar percentage of CMS (in the case of block copolymers represents the percentage within the functionalized block only).

Table 2. Molecular and Morphological Attributes of PS/S-Anth Polymers

notation	series	$N^{a,b}$	$f_{\text{func-PS}}{}^{b,c}$	$x^{b,d}$
PS/S-Anth(19,20%)		218		0.41
PS/S-Anth(25,50%)		357		0.73
PS/S-Anth(27:13,17%)	A	409	0.36	0.35
PS/S-Anth(27:13,25%)	A, B	416	0.37	0.47
PS/S-Anth(28:13,40%)	A	447	0.40	0.64
PS/S-Anth(27:20,25%)	B	507	0.49	0.47
PS/S-Anth(27:23,20%)	B	533	0.51	0.40
PS/S-Anth(27:26,22%)	B	575	0.55	0.43

[a] Volume-effective degree of polymerization (using PS repeat unit as the reference volume). [b] Calculated from M_n values of corresponding PS/CMS scaffolds, functionality content, and the respective densities of PS and homo-poly(S-Anth) (see Experimental Section). [c] Volume fraction of the functionalized blocks in the diblock copolymers. [d] Volume fraction of the Anth units in the functionalized block (i.e., volume-corrected functionality content).

Controlled free-radical polymerization techniques[15] were used to create "monoblock" random copolymer scaffolds, i.e., P(S-*co*-CMS), as well as diblock random copolymer scaffolds, i.e., PS-*b*-P(S-*co*-CMS). The molecular characteristics of these scaffolds are listed in Table 1. We denote the general monomer composition of these polymers as PS/CMS (regardless of whether they are monoblock or diblock copolymers) and identify the individual polymers by their number-averaged molecular weights (M_n) and the CMS content in molar percentage (given in parentheses and separated by a comma). In the case of diblock copolymers, the respective block lengths of the PS and functionalized PS blocks are given as $M_n{}^{PS}$:$M_n{}^{func-PS}$ (in place of the total M_n), and the CMS content corresponds to the functionalized block only. We note that for consistency usage of the term "functionality content" (and analogous terms) when regarding diblock copolymers always refers to the functionality content in the functionalized block only.

The chosen model functionality was 9-anthracene carboxylate (denoted as Anth), which features both steric bulk and some degree of interfunctionality interaction through aromatic stacking. Studies performed on a similar anthracene-modified PS in solution revealed that aromatic stacking between the anthracene units induces a folded chain structure;[16] part of the study presented in this paper is meant to probe such effects in the solid state. Figure 1 shows the structure of the Anth-functionalized polystyrenes, and Table 2 lists their molecular and morphological characteristics. Similar to the notation used for the PS/CMS scaffolds, we denote the Anth-functionalized polymers as PS/S-Anth, while the numbers in parentheses are equal to those used in the PS/CMS scaffolds (as both the scaffolds and the functionalized polymers share these respective attributes; CMS content is directly translated to Anth content).

The diblock copolymers used in this study form two fundamental series, which we denote A and B (see Tables 1 and 2). Series A is comprised of three polymers with structural characteristics of (27:13,17%), (27:13,25%), and (28:13,40%), in which the molecular weights in both blocks remains constant (within 1 kg/mol) while the functionality content is varied. This series thus allows the investigation of the influence of the functionality content parameter on the glass transition temperature, chain packing, and the effective incompatibility that leads to microphase separation. Series B, on the other hand, consists of four polymers having structural characteristics of (27:13,25%), (27:20,25%), (27:23,20%), and (27:26,22%), which are all made from the same batch of the first block (PS) and in which the functionality content is very similar. This series, therefore, allows qualitative probing of the contribution of varying polymer lengths (derived from changes in the functionalized block lengths) to the bulk periodicity of the microphase-separated melts at similar functionality content.

Experimental Section

Materials. All chemicals were reagent grade, purchased from Aldrich or Merck, and were used as received. Monomers (styrene and 4-chloromethylstyrene) were purified from the inhibitor either by distillation or by a short alumina plug.

Synthesis. P(S-*co*-CMS) and PS-*b*-P(S-*co*-CMS) polymer scaffolds were synthesized via nitroxide-mediated controlled free-radical polymerization.[15] In the case of diblock copolymers, the PS block was created first, purified by precipitation in methanol from remaining monomer, and then polymerization of the S/CMS mixture to yield the functionalizable block took place. Polymerizations of the functionalizable block were stopped at less than 10% conversion ratios to decrease the possibility of blockiness that may arise from the different reactivity ratios of styrene and CMS, 0.62 and 1.12, respectively.[17]

In a typical functionalization reaction, the parent polymer (1.0 CMS equivalent), 9-anthracenecarboxylic acid (1.1 equiv), and K_2CO_3 (1.5 equiv) were dissolved in a minimum volume of *N*,*N*-dimethylformamide (DMF) and stirred at 70 °C under an argon atmosphere overnight. Dropwise addition of water resulted in immediate precipitation. The light yellow solid was filtered, sonicated in methanol, filtered again, and dried under vacuum overnight (70−90% yield). Complete conversion (within NMR detection limits) was determined using side-chain CH_2 group resonance. When less than complete conversion was desired (for part of the DSC study as follows), substituent and base amounts were calculated accordingly, and the average conversion ratio was determined with NMR as described.

Characterization. Number-averaged molecular weights (M_n) and polydispersity indices (PDI) of the polymers in THF

solutions were determined from gel permeation chromatograms (GPC) acquired on an in-house built GPC system using PL Caliber data collection software, three-column set (Polymer Labs, Inc.; PLgel 5 μm columns, 300 × 7.5 mm, 10^3, 10^4, and 10^5 Å pore size), with an RI detector (Waters 403). The system was calibrated with respect to polystyrene standards (Polymer Labs, Inc.). CMS content was calculated according to ^{1}H NMR peak integration (using a Bruker AC-200 spectrometer operating at 200.13 MHz for ^{1}H) to an estimated error of ±5% CMS content. Glass transition temperatures were determined using differential scanning calorimetry (DSC), performed on ca. 10 mg samples under continuous nitrogen purge (50 mL/min) on a TA Instruments DSC 2910. Data represent the second heating cycles using a heating scan rate of 10 °C/min. Effective degrees of polymerization (N), statistical segment lengths (a), and volume fractions (f and x parameters) were referenced to a constant monomer volume of styrene ($v_0 = 164.5$ Å^3 according to $\rho_{PS} = 1.05$ g/mL).[17−19] The volume of Anth-modified styrene was estimated to be ca. 440 Å^3 as calculated from mass density measurement of the random copolymer PS/S-Anth(25,50%) (1.16 ± 0.01 g/mL, determined with a bubble-free pellet quenched from 150 °C using aqueous NaCl brines) under the assumption that the latter represents an algebraic average between the densities of PS and homo-poly(S-Anth).[20]

SAXS/WAXS Sample Preparation. Solid polymer samples (ca. 10 mg) in the precipitated powder form were placed in the center of a Kapton sheet, annealed at 150 °C under vacuum for 2 days, and quenched to room temperature.[21] All scattering experiments were performed at room temperature.

Wide-Angle X-ray Scattering (WAXS). Cu Kα X-rays (1.54 Å) served as the radiation source for WAXS and were used with a nickel filter. Images were recorded on 10 cm × 15 cm Fuji image plates using an evacuated Statton camera consisting of one pinhole collimator. The scattering patterns were scanned on a Fuji BAS-2500 image plate scanner; the resulting two-dimensional images were reduced to the one-dimensional form (I vs q) by angular integration, calibrated for camera length using Calcite, and corrected for Kapton scattering. Packing distances (d) were calculated from the respective maxima as $d = 2\pi/q$.

Small-Angle X-ray Scattering (SAXS). Cu Kα X-rays (1.54 Å) were generated in an Osmic MaxFlux source with a confocal multilayer optic (OSMIC, Inc.). Images were taken with a Molecular Metrology, Inc., camera consisting of a 3 pinhole collimation system, 150 cm sample-to-detector distance (calibrated using silver behenate), and a 2-dimensional, multiwire proportional detector (Molecular Metrology, Inc.). The entire X-ray path length was evacuated from the optic to the detector in order to reduce the background from air scattering. This setup allowed neglecting the correction for background scattering as proved by experiment. Two-dimensional images were reduced to the one-dimensional form using angular integration. Scattering vectors (q) were calculated from the scattering angles (θ) using $q = 4\pi \sin\theta/\lambda$, and domain periodicities (D) were calculated from the principal scattering maxima (q^*) using $D = 2\pi/q^*$.

Results and Discussion

Effect of Anth Side-Chain Groups on Glass Transition Temperatures. Glass transition temperature is one of the most essential properties of polymers, dictating important features such as thermomechanical behavior and processing conditions. In the context of microphase separation, for example, reaching the thermodynamically stable, microphase-separated structure requires overcoming the glass transition temperature (T_g) (either by annealing or by lowering the T_g by solvent vapor) to allow chain mobility.

The glass transition is a complex phenomenon that is not fully theoretically understood.[22] It is believed, however, that it is determined by the shape and bulkiness of the monomers and by intermolecular electrostatic interactions, as these factors strongly affect the

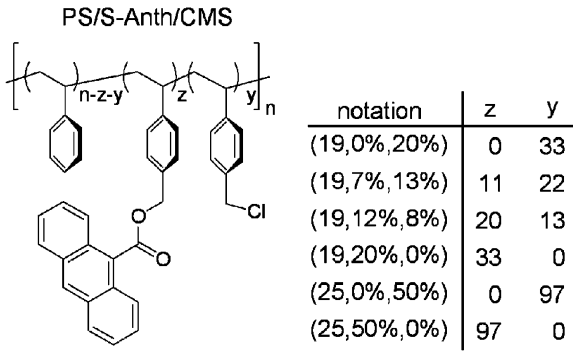

notation	z	y
(19,0%,20%)	0	33
(19,7%,13%)	11	22
(19,12%,8%)	20	13
(19,20%,0%)	33	0
(25,0%,50%)	0	97
(25,50%,0%)	97	0

Figure 2. Structure of partially Anth-functionalized monoblock copolymers (PS/S-Anth/CMS) featuring different modification ratios, from the parent PS/CMS scaffold (0% Anth content) to the fully converted PS/S-Anth (19,20%) and (25,50%).

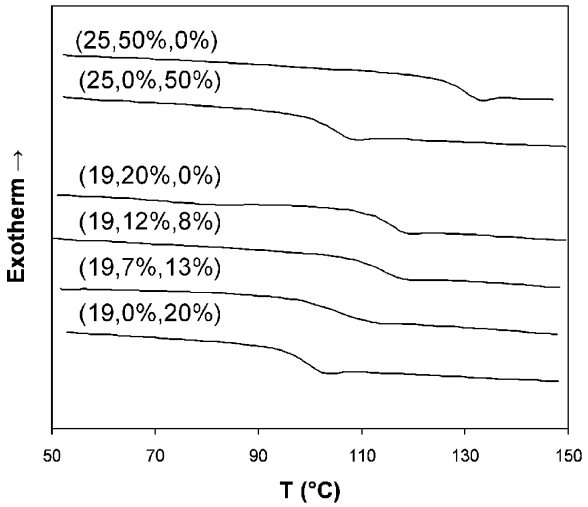

Figure 3. DSC curves of random copolymers PS/S-Anth/CMS derived from the PS/CMS scaffolds (19,20%) and (25,50%) at different conversion ratios of CMS units to Anth units. Curves are offset for clarity.

cooperative motion of the chain segments and hence the temperature at which the glass transition (that corresponds to reaching a certain free volume of the system) occurs. It is to be expected, therefore, that the rigid and bulky Anth functionality will cause an increase in T_g compared to that of pure PS. To probe this conjecture, we synthesized random copolymers PS/CMS (19,20%) and (25,50%), that are analogous in structure to the functionalized blocks in the diblock copolymer scaffolds used in this study (see Table 1). We compared between different modification ratios of the CMS units, from the unsubstituted parent copolymers PS/CMS to the fully Anth-converted PS/S-Anth copolymers (Figure 2; percentage values represent the respective molar percentages of Anth and CMS in the polymer). The corresponding DSC curves shown in Figure 3 demonstrate an obvious increase in T_g in both polymers with increasing average number of Anth units attached to the backbone.

It is well-known that in regular-sized polymers T_g is only weakly dependent on molecular weight[22] (and hence on total number of monomers). Therefore, the observed increase should be attributed to Anth functionality fraction (calculated on a volume basis[23]) rather than to the total number of Anth units. Figure 4 reveals a roughly linear relationship ($R^2 = 0.955$) between the determined T_g values and the calculated volume fraction of the Anth functionality (see Experimental Section). The effect of increasing T_g with increasing substitution

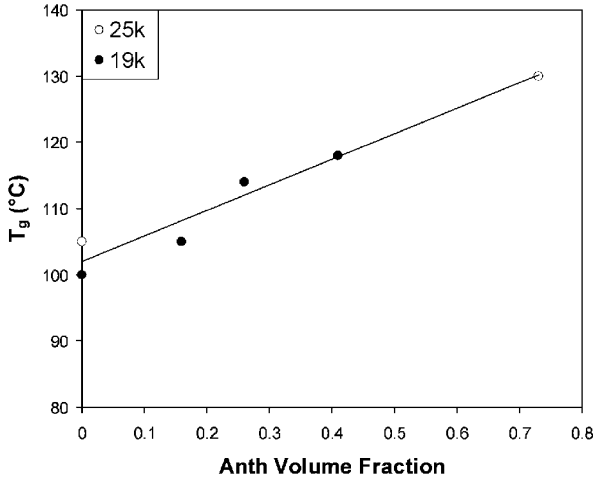

Figure 4. Relationship between glass transition temperatures and functionality volume fraction: black circles, PS/S-Anth/CMS series derived from PS/CMS (19,20%); open circles, PS/CMS and PS/S-Anth (25,50%) monoblocks.

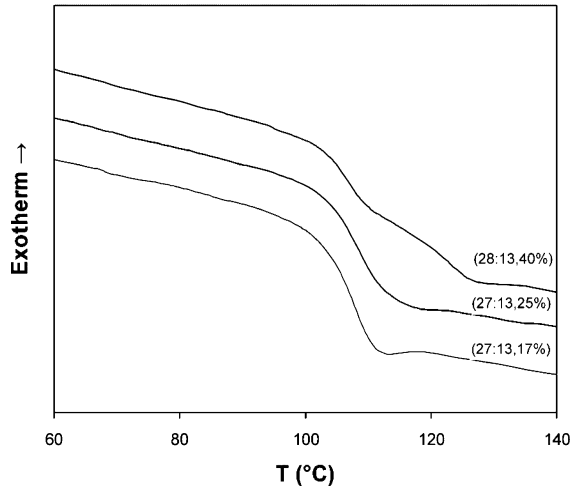

Figure 5. DSC curves of PS/S-Anth diblock copolymers of series A. Curves are offset for clarity.

ratio may originate both from the steric hindrance to the chains motion caused by the protruding bulky and rigid Anth groups and from enhanced interchain cohesion due to favorable aromatic stacking interactions between anthracene groups attached to different polymer chains and between anthracene groups and phenyl rings of the PS backbone.

A similar picture is observed for the diblock copolymers. As expected, the determined T_g values for the polymers of series B (featuring similar Anth content) are all within the range 108 ± 2 °C (not shown), evidencing the independence of T_g on total number of attached side-chain groups. The attenuation of the T_g compared to the corresponding PS/S-Anth (19,20%) monoblocks (118 °C) is a known phenomenon in block copolymers.[17] Figure 5 shows the DSC curves obtained for the polymers of series A, where the average molecular weights of respective PS blocks and the respective functionalized blocks remain constant while the Anth content in the functionalized block is changed. While the transitions associated with either block overlap at 108 °C for the low Anth content polymers, increasing the functionality content to 40% in PS/S-Anth (28:13,40%) creates a situation, in which the two transitions are clearly distinguishable [(107 °C of the PS block, 123 °C of the Anth-functionalized block]. This also

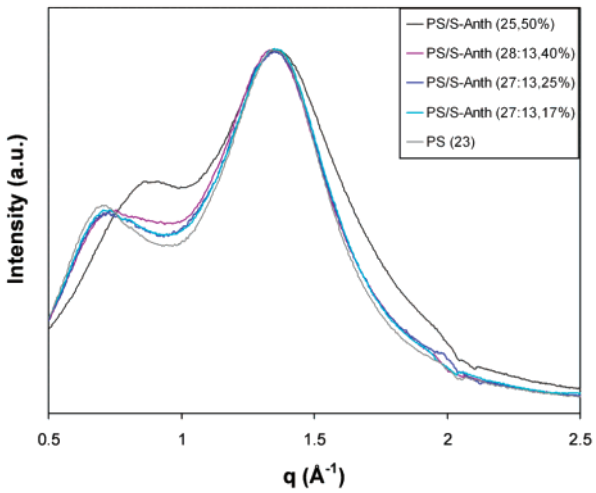

Figure 6. WAXS curves of PS-*b*-P(S-Anth) diblock copolymers of series A, and of PS (M_n 23K) and PS/S-Anth (25,50%), which represent the respective blocks in the diblock copolymers. Spectra are normalized to the most intense peak.

indicates the strong incompatibility between the two blocks in this polymer (vide infra).

Characterization of Internal Structure Using WAXS. Information about the internal melt structure can be obtained by wide-angle X-ray scaterring (WAXS), which reveals electron density correlations in the scattering angle range corresponding to the molecular scale. In Figure 6 we compare the WAXS curves obtained for polymers of series A with the curves obtained for PS (M_n 23K) and for PS/S-Anth (25,50%), which represent the respective PS and functionalized-PS blocks in the diblock copolymers.

Two main scattering maxima are observed in all curves. For PS, Mitchell and Windle proposed a "superchain" model to account for these two peaks.[24] According to their interpretation, the most intense peak (at q = 1.35 Å^{-1}, corresponding to a packing distance of 4.7 Å), which is also exhibited by samples of monomeric styrene and benzene, is attributed to phenyl ring packing (mainly from neighboring chains). This distance is slightly larger than that of stacking in simple aromatics due to the liquidlike ordering in the glassy polymer. The fact that this peak is common to all Anth-functionalized polymers corroborates this conclusion. The peak observed at lower q values (0.71 Å^{-1} for PS) appears only in polymerized styrenes and was termed by Mitchell and Windle the "polymerization peak".[24] In their "superchain" model they attributed it to the average packing distance between the "superchains" (8.8 Å for PS).

Comparison between PS and PS/S-Anth (25,50%) reveals in the latter a strong shift of the polymerization peak to a higher q value (0.91 Å^{-1}), which corresponds to denser chain packing (6.9 Å) compared to PS. We speculate that this indicates increased chain cohesion due to aromatic stacking of the anthracene groups, which is known for similar anthracene-functionalized polystyrenes in solution.[16] This result is also in accord with the increased mass density determined for PS/S-Anth (25,50%) compared to that of PS (1.16 and 1.05 g/mL, respectively). The observed line broadening in both peaks of PS/S-Anth (25,50%) compared to those of PS is attributed to the fact that the former is a copolymer, in which due to randomness the packing (at all levels) is naturally expected to be less well-defined than in a homopolymer.

The block copolymers show an intermediary behavior. As these polymers contain PS blocks as well as Anth-functionalized-PS blocks that exhibit smaller Anth content compared to that of PS/S-Anth (25,50%), the strongest scattering peak at $q = 1.35$ Å^{-1} resembles that of PS with only slight broadening observed. The polymerization peak, however, is slightly shifted toward higher scattering angles, and the curves seem to represent a convolution of three peaks [especially noticeable for the densely functionalized PS/S-Anth (28:13,40%)]: the regular phenyl ring packing at 1.35 Å^{-1} and two polymerization peaks (at 0.7 and 0.9 Å^{-1}) that correspond to the PS and functionalized-PS block, respectively. The WAXS dependence on the functionality content matches the picture observed in the DSC: while the curves of the less-functionalized diblocks almost exactly overlap, increase of the Anth content to 40% yields a marked change. It should be noted that the WAXS curves exhibited by the polymer of series B (not shown) also showed intermediary behavior (between that of PS and functionalized-PS monoblocks); nevertheless, these curves almost exactly overlapped, strengthening again the argument that the functionality fraction is more dominant over the total number of units in determining properties.

Characterization of Microphase Separation Using SAXS. Phase separation in polymeric systems arises from incompatibility between the polymers involved, which is characterized by Flory−Huggins incompatibility parameter χ.[25] In block copolymers, the covalent bond that connects between the two blocks prevents phase separation on a macroscopic scale and leads to the creation of periodic microdomains where the periodicity corresponds to the size of the block copolymer.[26] The morphology and the degree of microphase separation for a diblock copolymer with a given volume fraction of one of the blocks (f) is determined by the product χN, where N is the effective degree of polymerization. For perfectly symmetric diblock copolymers ($f = 0.5$), for example, mean-field theory predicts a critical value of 10.5 for the transition between disordered (homogeneous) phase and a microphase-separated structure.[27]

As the functionalized block in the PS/S-Anth diblock copolymers is not a homopolymer, the effective incompatibility (χ_{eff}) is not equal to pure incompatibility between styrene and Anth-modified styrene ($\chi_{\text{S,S−Anth}}$). Assuming a statistical distribution of the Anth groups in the functionalized block, the χ_{eff} is expressed in terms of the $\chi_{\text{S,S−Anth}}$ and the volume fraction of Anth in the functionalized block (x, see Table 2) as follows:[11]

$$\chi_{\text{eff}} = x^2 \chi_{\text{S,S−Anth}} \tag{1}$$

Equation 1 points to a strong dependence of the degree of microphase separation on the functionality volume fraction in the functionalized block. The degree of microphase separation can be determined experimentally using small-angle X-ray scattering (SAXS), which allows examination of the morphological structure of block copolymers in the bulk. Figure 7 shows the SAXS profiles obtained for the polymers of series A.[28] As expected from eq 1, small functionality content in the functionalized-PS block is not enough to render the two blocks incompatible; therefore, the SAXS profile of PS/S-Anth (27:13,17%) is featureless.[29] Increasing the Anth content to 25% already results in some degree of segregation manifested by a broad peak at $q = 0.28$ nm^{-1}. At 40% Anth content, the principal peak sharpens and the curve exhibits secondary scattering peaks, which reveal the expected slightly asymmetric ($f_{\text{func−PS}} = 0.40$) lamellar morphology.[30] It should be noted, however, that at this degree of functionalization it is reasonable to assume the existence of multiple block sequences of the Anth-functionalized styrene monomers; therefore, the effective incompatibility cannot be reliably calculated from eq 1 (which assumes statistical distribution of the comonomers).

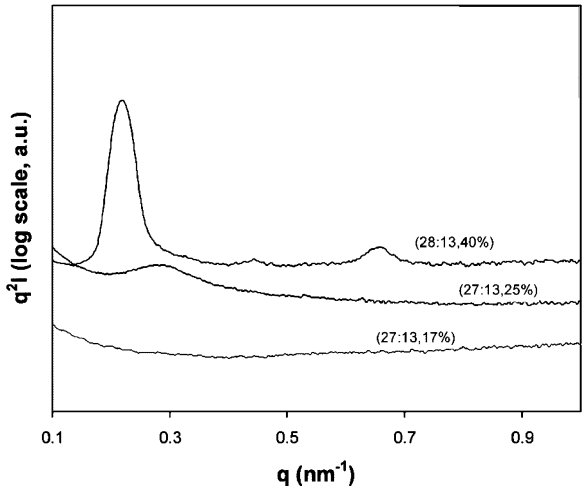

Figure 7. SAXS curves of series A of PS/S-Anth block copolymers, which feature different Anth content (in the functionalized blocks) with constant average degrees of polymerization. Curves are offset for clarity.

In general, an estimation of the incompatibility between two chemically distinct components of a copolymer can be obtained from the solubility parameters (δ_i) of the two blocks using eq 2:

$$\chi_{1,2} \approx (v_0/RT)(\delta_1 - \delta_2)^2 \tag{2}$$

where v_0 is a reference molar volume, R is the gas constant, and T is the temperature. The solubility parameter of a polymer can be calculated from the cohesive energy (E_{coh}) and the relationship

$$\delta = (E_{\text{coh}}/v)^{1/2} \tag{3}$$

where v is the molar volume of the respective polymer. For the estimation of E_{coh} we used a correlation developed by Bicerano[19] between topological indices and additive group contributions of Fedors,[31] which is useful for estimation of properties for uncommon polymers. The semiempirical estimate for $\chi_{\text{S,S−Anth}}$ is 0.103.[32] Experimentally, the effective incompatibility can be evaluated from the bulk periodicity (D) as follows:[33]

$$D = 1.10a\chi_{\text{eff}}^{1/6}N^{2/3} \tag{4}$$

where a is the average statistical segment length (calculated with respect to a reference monomer volume). Although eq 4 is strictly applicable only at the strong segregation limit ($\chi N > 100$), within reasonable error it is also useful for estimation of the effective incompatibility even for the cylindrical morphology and at the weak segregation regime.[34]

To obtain $\chi_{\text{S/S,Anth}}$ experimentally from eqs 4 and 1, we used the polymers of series B. These polymers

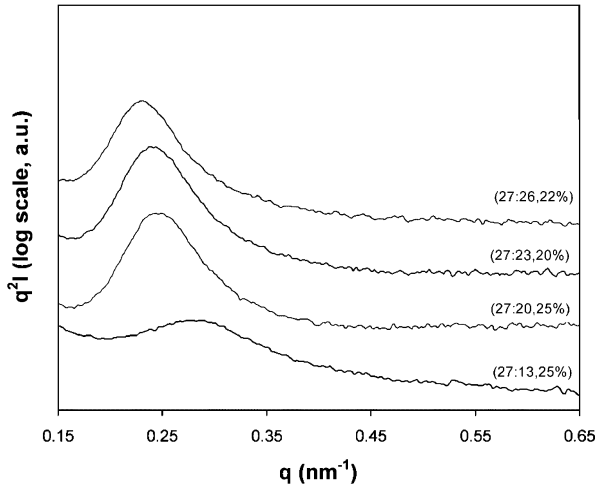

Figure 8. SAXS curves of series B of PS/S-Anth block copolymers, which feature increasing chain lengths at similar Anth content. Curves are offset for clarity

feature low Anth content and differ only in the length of the P(S-Anth) block (and hence in the total effective degree of polymerization N); therefore, they are suitable for the purpose. Owing to the consistency of conditions taken in the creation of this series,[35] we believe that this series affords a reasonable estimation of the $\chi_{S,S-Anth}$.

Figure 8 shows the SAXS profiles obtained for the polymers of series B,[28] from which a clear dependence is observed between the locations of the scattering maxima (corresponding to periodicities of 22.8, 25.4, 26.1, and 27.2 nm for the shortest to longest polymer, respectively) and the total polymer length. The shortest polymer, PS/S-Anth (27:13,25%), shows a broad and low-intensity peak, which indicates relatively weak segregation. This situation arises both from the fact that this polymer obviously exhibits the lowest value of $\chi_{eff}N$ due to its shortness and also from the fact that it is the most asymmetric polymer ($f_{func-PS} = 0.37$), for which the critical value $(\chi N)_{ODT}$ should be the highest in the series.

To extract $\chi_{S,S-Anth}$ from the SAXS data, the average statistical segment length (a) must be calculated for each polymer from the respective statistical segment lengths of styrene and Anth-modified styrene (a_S and a_{S-Anth}) as follows:[34]

$$a = \left(\frac{1 - f_{func-PS}}{a_S^2} + \frac{f_{func-PS}}{x a_{S-Anth}^2 + (1-x)a_S^2}\right)^{-1/2} \quad (5)$$

The statistical segment length of styrene (with respect to PS repeat unit as the reference volume) is 6.7 Å.[22] Steric hindrance created by the Anth side groups is expected to increase the chain stiffness compared to that of PS;[19] therefore, a_{S-Anth} is expected to by longer than a_S. Rigorously, the statistical segment length of a polymer is calculated from eq 6 using the polymer's density (ρ), its radius of gyration (R_g), and its molecular weight (M):

$$a^2 = 6N_{AV}\rho v_0(R_g^2/M) \quad (6)$$

where N_{AV} is Avogadro's number. Using the simplifying approximation that the ratio R_g^2/M is similar for PS and homo-poly(S-Anth) (and therefore scaling of a based on densities only), we estimate $a_{S-Anth} = 7.4$. Å, which is in line with the stiffness consideration mentioned above.

All four $\chi_{S,S-Anth}$ incompatibility values thus calculated from the periodicity values obtained from the SAXS data of polymer series B in combination with eqs 1 and 4−6 agree within $\chi_{S,S-Anth} = 0.11 \pm 0.02$. This value is in good agreement with the value of 0.103 calculated using topological indices.[19] The $\chi_{eff}N$ values calculated for this series fall within the range 11.0−11.6, which is in line with the apparent weak segregation in this series[36] evidenced by the absence of secondary SAXS peaks [compared, for example, with PS/S-Anth (28:13,40%)].

Conclusions

A series of polymer scaffolds that are amenable to functionalization were modified with 9-anthracene carboxylate functionalities and characterized using DSC, WAXS, and SAXS. It was found that the functionality content (in volume fraction terms) in the functionalized block is a dominant factor, affecting glass transition temperatures as well as structural properties such as chain packing and bulk periodicity in microphase-separated melts of diblock copolymers. Using SAXS, we were able to provide an estimate for the incompatibility parameter between styrene and Anth-modified styrene.

This study highlights the fundamental role of side-chain functionality in determining macromolecular behavior, particularly structural characteristics. Additionally, the approach presented in this paper offers the versatility of using the same polymer backbone for the attachment of different molecular entities, which provides a general framework for the study of structure−property relationship in polymers. Studies in this area are currently underway and will be reported in due course.

Acknowledgment. R.S. is in debt to Prof. Marc A. Hillmyer, Prof. Thomas P. Russell, and Matthew J. Misner for helpful discussions. Financial support from the NSF (MRSEC, DMR 0213695 and NIRT, DMI-0103024) is gratefully acknowledged. R.S. acknowledges The Fulbright Foundation for a postdoctoral fellowship.

Supporting Information Available: GPC traces and NMR spectra of all discussed polymers. This material is available free of charge via the Internet at http://pubs.acs.org.

References and Notes

(1) Decher, G. *Science* **1997**, *277*, 1232.
(2) Onitsuka, O.; Fou, A. C.; Ferreira, M.; Hsieh, B. R.; Rubner, M. F. *J. Appl. Phys.* **1996**, *80*, 4067.
(3) Donath, E.; Sukhorukov, G. B.; Caruso, F.; Davis, S. A.; Möhwald, H. *Angew. Chem., Int. Ed.* **1998**, *37*, 2202.
(4) Boal, A. K.; Ilhan, F.; DeRouchey, J. E.; Thurn-Albrecht, T.; Russell, T. P.; Rotello, V. M. *Nature (London)* **2000**, *404*, 746.
(5) Das, K.; Penelle, J.; Rotello, V. M. *Langmuir* **2003**, *19*, 3921. Duffy, D. J.; Das, K.; Hsu, S. L.; Penelle, J.; Rotello, V. M.; Stidham, H. D. *J. Am. Chem. Soc.* **2002**, *124*, 8290.
(6) Tripp, J. A.; Stein, J. A.; Svec, F.; Frechet, J. M. J. *Org. Lett.* **2000**, *2*, 195. Tripp, J. A.; Svec, F.; Frechet, J. M. J. *J. Comb. Chem.* **2001**, *3*, 216.
(7) Wang, J.; Kara, S.; Long, T. E.; Ward, T. C. *J. Polym. Sci., Polym. Chem.* **2000**, *38*, 3742.
(8) Thurn-Albrecht, T.; Schotter, J.; Kästle, C. A.; Emley, N.; Shibauchi, T.; Krusin-Elbaum, L.; Guarini, K.; Black, C. T.; Tuominen, M. T.; Russell, T. P. *Science* **2000**, *290*, 2126. Chan, V. Z.-H.; Hoffman, J.; Lee, V. Y.; Iatrou, H.; Avgeropoulos, A.; Hadjichristidis, N.; Miller, R. D.; Thomas, E. L. *Science* **1999**, *286*, 1716. Park, M.; Harrison, C.; Chaikin, P. M.; Register, R. A.; Adamson, D. H. *Science* **1997**, *276*, 1401.
(9) Bendejacq, D.; Ponsinet, V.; Joanicot, M.; Vacher, A.; Airiau, M. *Macromolecules* **2003**, *36*, 7289.

(10) Ruokolainen, J.; Mäkinen, R.; Torkkeli, M.; Mäkelä, T.; Serimaa, R.; ten Brinke, G.; Ikkala, O. *Science* **1998**, *280*, 557. Ikkala, O.; ten Brinke, G. *Science* **2002**, *295*, 2407.
(11) The effect of an atom substitution on the phase behavior of polymers was investigated in blends. See, for example: Jablonski, E. L.; Gorga, R. E.; Narasimhan, B. *Polymer* **2003**, *44*, 729. Gorga, R. E.; Jablonski, E. L.; Thiyagarajan, P.; Seifert, S.; Narasimhan, B. *J. Polym. Sci., Part B: Polym. Phys.* **2002**, *40*, 255. Alberda, G. O. R.; Meyboom, R.; ten Brinke, G.; Ikkala, O. *Macromolecules* **2000**, *33*, 3752. Oudhuis, A. A. C. M.; ten Brinke, G.; Karasz, F. E. *Polymer* **1993**, *34*, 1991. Salomons, W.; ten Brinke, G.; Karasz, F. E. *Polym. Commun.* **1991**, *32*, 185.
(12) Ring-opening metathesis polymerization (ROMP) provides an exception in the sense that it is relatively tolerant to a wide variety of preexisting monomer functionality. See, for example: Schwab, P.; Grubbs, R. H.; Ziller, J. W. *J. Am. Chem. Soc.* **1996**, *118*, 100. Lynn, D. M.; Kanaoka, S.; Grubbs, R. H. *J. Am. Chem. Soc.* **1996**, *118*, 784. Wu, Z.; Nguyen, S. T.; Grubbs, R. H.; Ziller, J. W. *J. Am. Chem. Soc.* **1995**, *117*, 5503. Hillmyer, M. A.; Laredo, W. R.; Grubbs, R. H. *Macromolecules* **1995**, *28*, 6311. Stumpf, A. W.; Saive, E.; Demonceau, A.; Noels, A. F. *J. Chem. Soc., Chem. Commun.* **1995**, 1127. Fraser, C.; Grubbs, R. H. *Macromolecules* **1995**, *28*, 7248.
(13) See, for example: Lee, H. J.; Nakayama, Y.; Matsuda, T. *Macromolecules* **1999**, *32*, 6989. Worl, L. A.; Jones, W. E., Jr.; Strouse, G. F.; Younathan, J. N.; Danielson, E.; Maxwell, K. A.; Sykora, M.; Meyer, T. J. *Inorg. Chem.* **1999**, *38*, 2705. Park, Y. H.; Shin, H. C.; Lee, Y.; Son, Y.; Baik, D. H. *Macromolecules* **1999**, *32*, 4615.
(14) Dependent on the functionality, at high CMS:S ratios some processing parameters such as solubility and the ability to achieve complete postpolymerization functionalization become problematic.
(15) Benoit, D.; Chaplinski, V.; Braslau, R.; Hawker, C. J. *J. Am. Chem. Soc.* **1999**, *121*, 3904. Harth, E.; Hawker, C. J.; Fan, W.; Waymouth, R. M. *Macromolecules* **2001**, *34*, 3856. Hawker, C. J. *J. Am. Chem. Soc.* **1994**, *116*, 11185.
(16) Ilhan, F.; Gray, M.; Blanchette, K.; Rotello, V. M. *Macromolecules* **1999**, *32*, 6159.
(17) *Polymer Handbook*, 4th ed.; Brandrup, J., Immergut, E. H., Grulke, E. A., Eds.; Wiley-Interscience Publication: New York, 1999.
(18) Van Krevelen, D. W. *Properties of Polymers: Their Correlation with Chemical Structure; Their Numerical Estimation and Prediction from Additive Group Contributions*, 3rd ed.; Elsevier: Amsterdam, 1990.
(19) Bicerano, J. *Prediction of Polymer Properties*, 3rd ed.; Marcel Dekker: New York, 2002.
(20) The calculated value of 1.27 g/mL for the mass density of homo-poly(S-Anth) is in reasonable agreement with the value 1.23 g/mL obtained from semiempirical calculations using the topological approach (connectivity indices).[19] We find that within this range the variation of our quantitative results is marginal (e.g., volume fractions vary by about 1%).
(21) In general, we refrained from casting the samples from solution to avoid kinetic entrapment effects caused by selectivity of the solvent to either block. Nevertheless, we note that annealed samples cast from toluene still exhibited the same SAXS characteristics as those annealed from the powder form, which therefore leads us to believe that the investigated melts were in equilibrium.
(22) *Physical Properties of Polymers Handbook*; Mark, J. E., Ed.; American Institute of Physics: Woodbury, NY, 1996.
(23) In these calculations we neglected the difference between CMS and styrene. Calculated volume fractions of the Anth functionality in PS/S-Anth/CMS (19, 7%, 13%) and (19, 12%, 8%) are 0.16 and 0.26, respectively. For data pertaining to the fully converted PS/S-Anth (19, 20%) and (25, 50%) see Table 2.
(24) Mitchell, G. R.; Windle, A. H. *Polymer* **1984**, *25*, 906.
(25) Strobl, G. *The Physics of Polymers*; Springer: Berlin, 1996.
(26) Fredrickson, G. H.; Bates, F. S. *Annu. Rev. Mater. Sci.* **1996**, *26*, 501. Bates, F. S.; Fredrickson, G. H. *Annu. Rev. Phys. Chem.* **1990**, *41*, 525.
(27) Leibler, L. *Macromolecules* **1980**, *13*, 1602.
(28) The SAXS curves are plotted as q^2I vs q (instead of I vs q) under the assumption that the polymers feature lamellar morphology, based on the range of calculated volume fractions of the functionalized blocks (0.36−0.55) and mean-field theory.
(29) This situation does not result from lack of electron density contrast that may arise from a small number of Anth functionalities in the PS/S-Anth (27:13, 17%) polymer; other polymers that feature the same low functionality content but longer functionalized blocks (with up to twice the total number of Anth units per polymer) do not exhibit a distinct SAXS peak as well.
(30) The existence of the small scattering peak at $q = 0.56$ nm^{-1} ($2q^*$) is indicative of the slight volume fraction asymmetry calculated for this polymer ($f_{\mathrm{func-PS}} = 0.40$), as in perfectly symmetric diblock copolymers it is completely absent.
(31) Fedors, R. F. *Polym. Eng. Sci.* **1974**, *14*, 147. Fedors, R. F. *Polym. Eng. Sci.* **1974**, *14*, 472.
(32) For consistency, all the variables appearing in eqs 2 and 3 were also evaluated using the topological indices.
(33) Semenov, A. N. *Sov. Phys. JETP* **1985**, *61*, 733.
(34) For a detailed discussion and references, see: Ren, Y.; Lodge, T. P.; Hillmyer, M. A. *Macromolecules* **2000**, *33*, 866. Ren, Y.; Lodge, T. P.; Hillmyer, M. A. *Macromolecules* **2002**, *35*, 3889.
(35) All precursors to polymers of series B were synthesized from the same batch of PS block, with exactly the same styrene/CMS mixture composition (i.e., comonomer quantities); thus, the differences between the functionalized blocks of these polymers resulted only from different polymerization times.
(36) Despite the lack of secondary scattering peaks in the SAXS curves of the polymers of series B, we consider the melts of these polymers, quenched from 150 °C, as phase-separated, since only weak dependence of the scattering behavior on annealing temperature or annealing scheme was observed. For example, annealing at 150 °C for a few hours, then at 125 °C for 2 days, and then slowly cooling the samples to room temperature did not result in a significant change in the principal peak location/width or appearance of secondary scattering peaks. Therefore, the absence of secondary scattering peaks is attributed to weak segregation (and possibly also to low electron density contrast) rather than to disorder.

MA035488D